Journal of Signal Processing Systems
https://doi.org/10.1007/s11265-023-01837-z

Calibrating a Three-Viewpoints Thermal Camera with Few Correspondences

Ju O Kim[1] · Jieun Kim[1] · Deokwoo Lee[1]

Received: 7 September 2022 / Revised: 2 January 2023 / Accepted: 2 January 2023

Abstract
This paper proposes the approach to calibration of a thermal camera that has three viewpoints. This work estimates the intrinsic parameters of the camera by establishing geometric relationship between real-world scene points and image points. This work estimates the extrinsic parameters, i.e., rotation and translation of the camera using vanishing points. The present work is different from the existed work on the calibration from three perspectives. The first one is that this work calibrates thermal camera with three viewpoints whose relative rotation is greater than 180-degree. The second one is that the viewpoints shares few overlapped areas due to the structure of the camera, so the proposed work is more challenging and difficult than the previous work on the calibration. The third one is that projected image of a scene requires quality enhancement for the calibration. Since few overlapped images are given *a priori*, feature matching cannot be used for the calibration. Instead of using correspondence matching, vanishing points are exploited to estimate relative rotations of cameras. The intrinsic parameters are estimated by capturing thermal-checkerboard followed by image processing. Experimental results show the accuracy and stability of the proposed approach for estimation of the intrinsic and the extrinsic parameters.

Keywords Thermal camera calibration · Few correspondences · Rotation · Translation · Intrinsic parameters · Vanishing points

1 Introduction

Knowledge about geometric relationship between viewpoints that are located at different positions has been one of the most fundamental and crucial factors in the areas of computer vision, especially in depth camera system. Depth camera has lone been of interest in computer vision because it provides rich information about three dimensional(3D) coordinates of real world scenes. In computer vision, estimation of depth of a 3D scene or object is one of the most important problems and numerous algorithms have been introduced. To achieve accurate depth information of 3D target scene, two main approaches are usually employed, the one is passive and the other one is active method.

In the passive method, multiple viewpoints acquire 2D image of 3D scene, and all of the viewpoints capture the same 3D target. Multiple 2D images of the same scene can provide sufficient information about 3D coordinates of the target scene. In the passive method, to achieve accurate result of depth estimation, image acquisition, feature extraction, feature matching, etc., should be appropriately carried out [1]. In the active method, different from the passive method, passive sensor (usually camera) and light source are employed for depth estimation. Light source usually generates specific shape, called light pattern, and shape of 3D object surface deforms the light pattern. The deformation provides information about 3D coordinates of the target object [2]. In the active method, binary pattern, color pattern, coded pattern, phase information of light source, etc., have been popularly used to estimate depth value of a point on the object surface [3]. In the active method, accurate acquisition of an image of deformed light patterns, knowledge about the original light patterns, detection of the light patterns, etc., are the most important parts to achieve

✉ Deokwoo Lee
dwoolee@kmu.ac.kr

Ju O Kim
monkey4650@gmail.com

Jieun Kim
lilly9928@icloud.com

[1] Department of Computer Engineering, Keimyung University, Daegu 42601, Republic of Korea

Published online: 20 January 2023

reliable results of depth estimation. Both of the passive and the active methods requires accurate and stable calibration results.

Prior to estimation of depth of a target scene, accurate information about relative locations of cameras (in the passive method) or relative location between a camera and a light source (in the active method) is strongly desired. In addition, internal characteristics of a camera also contributes to accurate calculation of depth values. Once camera is calibrated, the relative locations of the components (e.g., camera and light source) and internal parameters of cameras are known or estimated. Relative location is composed of relative rotation and translation of cameras. Relative location is called external characteristics of cameras. In other words, camera calibration is estimating (or finding) the external and the internal camera parameters.

Camera calibration is one of the most important procedures in depth estimation or 3D reconstruction. In this section, we chiefly introduces the calibration of stereo vision system that is one of the passive methods using two cameras, because this work uses three-viewpoints camera system whose calibration basically obeys the same principle that is employed in stereo camera system.

As very well known, calibration algorithm has been investigated in the areas of computer vision since 1970's. However, the method introduced in 1970s used special cameras for the calibration and there were many unknown parameters to be solved (17 unknown ones). In Tsai's work in 1987, pattered object (chessboard pattern) is used for a calibration, and the planar object with special patterns is captured by multiple viewpoints. The approach is one of the techniques that are currently employed in practice. 2D images of the planar object are used to estimate the intrinsic and the extrinsic parameters. Multiple-view images of the patterned object are collected by multiple veiwpoints that are located at different positions. Multiple number of captures from different locations is considered a standard approach to camera calibration since Tsai's algorithm has been introduced. In addition to estimation of the parameters, horizontal scaling factor and lens distortion (distortion parameters) are estimated, and these are also one of the optimization problem. Tsai proposes the approach to camera calibration using linear least-square fitting methods.

In 1990s and early 2000s, there have been remarkable improvements on calibration techniques; more precise and more efficient approaches have been introduced. In the late 1990s, Zhang proposes the approach-this work is considered on of the most popular algorithm for the calibration-to the calibration using chessboard patterned objects and the approach provides accurate and stable results of parameter estimation [5]. Once homography matrix ($\mathbf{H} \subset \mathbb{R}^{3\times3}$) is estimated between 3D planar object and projected 2D image, the intrinsic and the extrinsic camera parameters are estimated in linear manner. Zhang's work also takes into account lens distortion. Faugeras, in the late 1980s and the early 1990s, proposed the calibration technique that does not use special patterned object for calibration [6]. Here, *epipolar constraint* is fully exploited based on geometric relationship between cameras and 3D target scene. Hartely, in 1990s, contrary to the work by Faugeras, proposed the approach to the calibration problem by using correspondence matching, instead of using epipolar geometry [7]. Hartely's work focuses on both of stationary and rotating cameras, and also focuses on solving rectification problem [7]. Four step calibration that has considered image distortion and used circular patterns has been introduced by Heikkilä [8]. This work uses circular patterns instead of rectangular ones. Projection of 3D image points to 2D image plane results in distortion of the circular patterns, and geometric and mathematical modeling of the distortion and correction plays a key role to estimation of the intrinsic and the extrinsic camera parameters. Recently, deep neural network has been employed to the calibration problem [9]. The approaches aforementioned basically obey geometric characteristics of cameras, 3D objects and images in 2D image plane. For non-overlapping calibration, an approach is proposed to extract external parameters using moving objects. [10]

In this paper, we propose the approach to estimating the intrinsic and the extrinsic parameters of thermal camera with three lenses. Different from the existed method, this work deals with challenges; The first one is that structure of camera system is totally different from general structure of stereo camera system. The second one is that the cameras does not share common image points as conventional stereo vision system fully exploits feature points that belong to all of the viewpoints that enable us to perform feature matching for disparity estimation. Since no features are commonly included in 2D images planes of the cameras, we try to generate artificial planar images of the same patterns that are used for the calibration, i.e., chessboard pattern. In other words, our work aims at camera calibration under the incomplete circumstances compared to existed work of the calibration. The challenges of this paper is twofold : first to present a solution for the calibration problem of thermal camera system with three viewpoints that cannot share common feature points, and second to validate the proposed method can provide reliable calibration result by generating artificial planar images with rectangular patterns that are used for the calibration.

The rest of this paper is organized as follows. Section 2 describes related work of camera calibration. This section introduces calibration algorithms that have been popularly used in the areas of computer vision. The section also introduces related work of calibration of thermal camera system. Section 3 shows overall procedure of the proposed approach in this paper, and also shows system architecture of the camera

that to be calibrated in this paper. Sections 4 and 5 describes the method of the calibration of thermal camera, and these are the most important contribution in this paper. Section 6 shows experimental results to substantiate the proposed approach. Section 7 provides conclusion remarks and future research plan.

2 Related Work

2.1 Camera Calibration

As mentioned above, once camera is calibrated, we have two sets of parameters, the one is the intrinsic (or internal) and the other one is the extrinsic (or external) parameters. The intrinsic parameters are composed of the focal length (f) of a camera, skewness factor (s) and principal points ($\mathbf{p}$) of 2D image (p_x and p_y). The extrinsic parameters are composed of rotation ($\mathbf{R}$) and translation ($\mathbf{t}$). $\mathbf{R}$ and $\mathbf{t}$ are relative rotation and distance between optical centers, respectively. To achieve accurate depth of 3D target scene from a set of 2D image, the calibration parameters should be estimated *a priori*. To mathematically model camera calibration, pinhole camera model is assumed in this paper, and projection of 3D point ($\mathbf{M} \in \mathbb{R}^3$) in a real world scene to 2D point ($\mathbf{m} \in \mathbb{R}^2$) is written by

$$\mathbf{m} = \mathcal{P}\mathbf{M}, \tag{1}$$

where $\mathcal{P}$ represents transformation (projective transformation here) between 3D space and 2D space. Camera calibration aims at finding all of the elements of a matrix $\mathcal{P} \subset \mathbb{R}^{3\times4}$. Thus, homogenious coordinate system is employed for projective transformation. $\mathcal{P}$ can be decomposed into the intrinsic and the extrinsic parameters as follows;

$$\mathcal{P} = \mathbf{M}_{\text{in}}\,\mathbf{M}_{\text{ex}}, \tag{2}$$

where $\mathbf{M}_{\text{in}}$ and $\mathbf{M}_{\text{ex}}$ represent the matrices of the intrinsic and the extrinsic parameters, respectively. $\mathbf{M}_{\text{in}} \subset \mathbb{R}^{3\times3}$ can be represented as follows;

$$\mathbf{M}_{\text{in}} = \begin{bmatrix} \alpha_x f_x & s & p_x \\ 0 & \alpha_y f_y & p_y \\ 0 & 0 & 1 \end{bmatrix} \tag{3}$$

where f_x and f_y are focal length of horizontal and vertical direction, respectively, α_x and α_y are aspect ratios (or scale factor), respectively, and $f_x = f_y$ is usually assumed in practice. If the calibration results show different values, $(f_x + f_y)/2$ is also used in practice. $\mathbf{M}_{\text{ex}} \subset \mathbb{R}^{3\times4}$ is composed of the rotation $\mathbf{R}$ and the translation ($\mathbf{t}$) as follows;

$$\mathbf{M}_{\text{ex}} = [\mathbf{R}|\mathbf{t}] = \begin{bmatrix} r_{11} & r_{12} & r_{13} & t_x \\ r_{21} & r_{22} & r_{23} & t_y \\ r_{31} & r_{32} & r_{33} & t_z \end{bmatrix}, \tag{4}$$

where $\mathbf{R}$ is 3×3 rotation matrix and $\mathbf{t} = [t_x, t_y, t_z]^T$ is a translation vector. By using *Rodriguez transformation*, $\mathbf{R}$ can be represented as 3×1 vector composed of rotation values in x, y and z direction. Concerning all above, in computer vision, camera calibration work aims at finding $\mathbf{M}_{\text{in}}$ and $\mathbf{M}_{\text{ex}}$. From mathematical perspectives, calibration can be formulated as optimization problem. To achieve precise calibration result, lens distortion needs to be taken into account in addition to solving Eq. (2). There have been extensive research work on accurate modeling of lens distortion which is usually modeled in nonlinear manner [4]. To summarize, camera calibration work can be decomposed into three sub-tasks; estimating the internal and the external parameters, and modeling lens distortion.

2.2 Vanishing Point Based Calibration

This section presents related research to the work proposed in this paper, camera calibration using vanishing points(VPs). VP based camera calibration is on the basis of the properties that parallelism in 3D real world space may not preserved in 2D space Fig. 1.

VP based camera calibration have been of interest since early 1990s. In 1980s, Tsai's calibration using the calibration object has been one of the most used methods. Although VPs are not explicitly used in the work of Haralick [11], the main idea is very simiar to the method using VPs in that geometric relationship between a perfect rectangle and quadrangle that is a projected image of the rectangle is employed. Since a rectangle has two pairs of parallel lines, projection of the rectangle may not preserve parallelism in 2D image plane anymore. In this work, only rotation of a camera is determined. The work of Caprile and Torre [12] and of Shigang et al. [13] are considered the first papers that propose the approach to camera calibration using vanishing points(VPs). In [13], the intrinsic parameters of a camera is estimated on the basis of using a unique association between parallel lines and the corresponding ideal point that is defined as the intersection position of parallel lines (parallel lines intersect at infinity

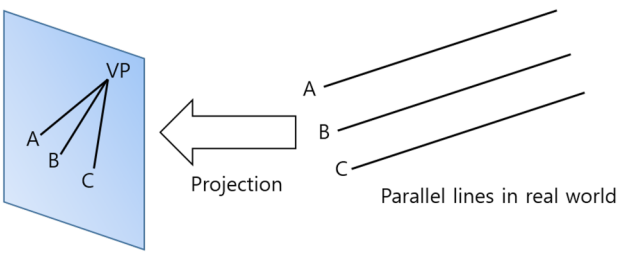

Figure 1 VP based camera calibration employs the concept that parallel lines intersect at the point of infinity, and the infinity point is projected on to the vanishing point in 2D space.

and this is called *ideal point*). On the basis of the properties of vanishing lines, the work estimates principal points and focal length. In this work, for estimation of the intrinsic parameters, experiments are conducted using calibration plane and dimension of the plane is known. The work reports that three images of the plane are required if aspect ratio is not known *a priori*. In the work of [12], it exploits VPs to estimate the intrinsic and the extrinsic parameters. The work is composed of two steps; the first one is to estimate focal length, principal points using an image of single cube, and the second one is to estimate the relative orientation and position of cameras using an image of a pair of planar pattern, and the matching of VPs provide sufficient information to calculate rotation matrix followed by estimation of translation using triangulation. Contrary to the approaches aforementioned, real images are used for camera calibration. Shigang et al. [13] proposed the approach to estimating change of camera azimuth using VPs extracted from horizontal lines. In this work, a single camera embedded to a robot moves with known velocity and focal length, and non-parallel horizontal lines are utilized. Focal length is assumed to be known *a priori*, and the robot and the camera moves in horizontal direction. Although there are many constraints in the proposed approach, this is also considered among the beginning stages of the calibration using VPs, particularly of rotation angle of a camera. Guillou et al. [14] proposed the approach to camera calibration using VPs from a single image. In this work, instead of using calibration object e.g., patterned object, and the proposed method applies to various real images. The work reports that two VPs from single image is enough to estimate the intrinsic and the extrinsic parameters except aspect ratios are assumed to be fixed by users. In addition to the calibration, the work also provides coarse 3D reconstruction results. Chen and Jiang [15] used a calibration object having a grid to determine a camera location by detecting horizontal and vertical parallel lines followed by extracting VPs. Statistical method has been employed to achieve a resolution of subpixel level. In the work of Wang and Tsai [16], the intrinsic and the extrinsic parameters are determined by using vanishing lines from calibration object. Calibration object is a shape of planar hexagon, and six edge points are firstly extracted followed by placing three pairs of parallel lines. The result of the calibration shows better accuracy compared to the work of similar approach that uses triplet of lines in the image [17]. This paper reports that accuracy of VP detection plays an important role to the calibration results. Cipolla et al. [18] also proposed the approach to the calibration using VPs, and the work also uses real images, real architectural scenes. In this work, three mutually orthogonal directions are exploited to achieve the intrinsic and the extrinsic parameters. This work also provides, in addition to the calibration, 3D reconstruction, rendering and texture mapping. In the work of Orghidan et al. [19] proposed VP based estimation of the intrinsic and the extrinsic parameters using two or three VPs from known patterns, such as two orthogonal checkerboard patterns. Lee and Yoon [20] proposed VP based estimation of camera based on sequential Bayesian filtering. This work starts from the motivation that Manhattan world constraint does not always apply to real world scenes. Thus, this work does not require the Manhattan world constraint. The work does not require orthogonality of VPs, so it detects and removes parallel lines and VPs, these are different from the previous work that uses Manhattan world constraint [21–23] The proposed approach performs real time estimation of a camera orientation and shows robustness to noise and limited scene constraints.

This paper also fully exploits VPs from checkerboard patterns, but the proposed work in this paper is different from the existed work in that the present work deals with a calibration of a three-view thermal camera, and any prior information about positions of a camera or checkerboard is not provided. Since a thermal camera is used, acquired image of a checkerboard needs to be enhanced. Thus, pre-processing of an acquired image is required in this work. Recently, calibration has been performed using lines that project into circles in 2D image plane [24]. Two orthogonal VP model and LCC(line of circle centers) provide information to find the intrinsic and the extrinsic parameters. This work assumes that lines in the scene is a short circular arc in the image plane due to a radial distortion of a lens, and the circular fitting can be carried out to estimate center and amount of lens distortion, focal length and camera orientation. This work, of course, can suffer from accomplishing perfect circular fitting in 2D image plane. The assumption that parallel lines in 3D space defines a line in a circle in 2D image plane may not always work for all of the real scene. VP based calibration unexpectedly suffers from the error of VP localization. Refinement of VPs detection, hence, can increase accuracy of VP localization, to this end, calibration accuracy is also can be improved. Previous works has focused on accurate VP detection that enables significant improvement of calibration results [25, 26]. Online calibration estimates camera orientation in real time manner in practical perspectives, e.g., ADAS(advanced driver assistance system). Since cameras are mounted on a vehicle, its orientation can be changed due to vibration or other external impact. Based on the acquired frames of images, motion based VPs detection is carried out for the calibration. Usually, the intrinsic parameters of a camera is determined in manufacturing process [27]. VP based camera calibration work is still challenging because higher accuracy and speed are desired in various environments [28].

2.3 Calibration with Non Overlapping Areas

In computer vision and related applications, calibration of a set of cameras with non-overlapping views is one of the challenging tasks. In the course of depth estimation using multiple-view cameras, e.g., stereo camera system, all of the viewpoints share the same feature points included in the real world objects. We define the areas that have the same feature points as overlapping areas. With overlapping areas, projected image of the real world scene provides sufficient information to provide depth information of the target scene. In other words, without overlapping areas, one suffers from low accuracy of camera calibration. Low accuracy of calibration results in low quality of depth estimation. Despite of difficulties of achievement of calibration result without overlapping areas, numerous research activities have been performed to gain highly accurate calibration result. In general, although cameras are extremely disjointly located, intrinsic parameters can be estimated using standard(or conventional) approach. However, estimation of the extrinsic parameters(rotation and translation vectors) is a difficult task. With the condition of non-overlapping field of view, there have been research activities in three categories. The first one is using static camera without additional information. In this case, the calibration suffers from low accuracy or it sometimes is impossible. The second one is using moving camera. Since the camera is moving, it is possible to create overlapping field of view. While a camera is moving, calibration objects need to be accurately tracked, and a relative speed of a moving camera needs to be known *a priori* [29]. In the case of using two or more cameras, rigidity constraint also can be additional information for the calibration. In this case, trajectory of a camera is required [30]. Recently, augmented reality(AR) marker has been added to find transformation between the marker and a camera, to this end, relative orientation of a camera can be calculated. The third one is to use additional information or an additional equipment. VP can be an example of technologies with additional information. To fully exploit VP, a set of straight lines (some of them should be parallel in real world space) belong to real world scene. A mirror can be an example of an additional equipment that can create overlapping field of view. Using a mirror, it is possible to create different viewpoints, then overlapping field-of-view can be achieved [31]. Gray code pattern has been used to alleviate limitation of non-overlapping conditions [32]. In the fields of robotics, camera with non-overlapping camera rig, camera calibration has been carried out by maneuvering the camera system while it observes a target scene [33], or by moving the robot for acquisition of real-world scene [34]. SAM(structure and motion) algorithm can be another possible approach to estimation of relative rotation and orientation of cameras. In the case of nonoverlapping viewpoints, it is inevitable to use additional information, additional constraints (or assumption) or additional equipments have been used to provide accurate calibration results. In addition to the previous work aforementioned, state-of-the-art calibration with non-overlapping areas can be also found in [35].

3 Overall Architecture

This section briefly introduces overall flow diagram of the proposed approach for three-view thermal camera system. As aforementioned, the camera has three viewpoints each of which has different orientation. The viewpoints have different and relative rotations and translations each other. Fig. 2 show a camera that is used in this work.

As shown in Fig. 2, a camera has three viewpoints, and contrary to usual depth camera systems (e.g., stereo camera), relative rotation angle is greater than 180° (degree) (240° (degree) between viewpoints). The camera used in the experiment was thermal camera which is different from general stereo camera. In addition, the manufactured camera has almost no overlapping views, especially in a multi-camera system, the angle between views exceeds 180 degrees. So in this case, the experiment environment is very different from a stereo camera, and because of the non-overlapping viewpoints it leads to difficulties in depth estimation. However, this paper proposes the approach to find the external and the internal camera parameters that can be used for depth estimation, 3D reconstruction, etc. Fig. 3 shows overall flow diagram of contribution of this paper.

Calibration starts from capturing a calibration object. There is no restriction on selecting calibration object, but some patterned ones are usually used. Some calibration methods use real object in 3D domain, by using epipolar constraints. However, calibration using patterned objects are still considered accurate and stable because structure and information of the object is known, and this information enables us to achieve more accurate calibration results. In this paper, we also use checkerboard patterned object whose visual quality is varying with applied temperature to the object (Fig. 4).

Since applied temperature affects to quality of images, we need to find optimal temperature so that the next procedures

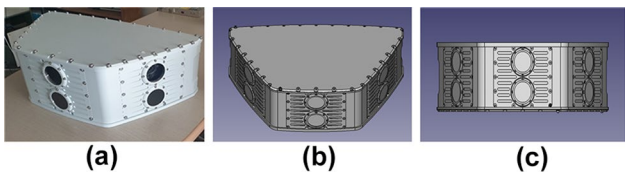

Figure 2 Three-viewpoints thermal camera system. **a** Thermal three view camera. **b** and **c** A structure of the camera from different viewpoints.

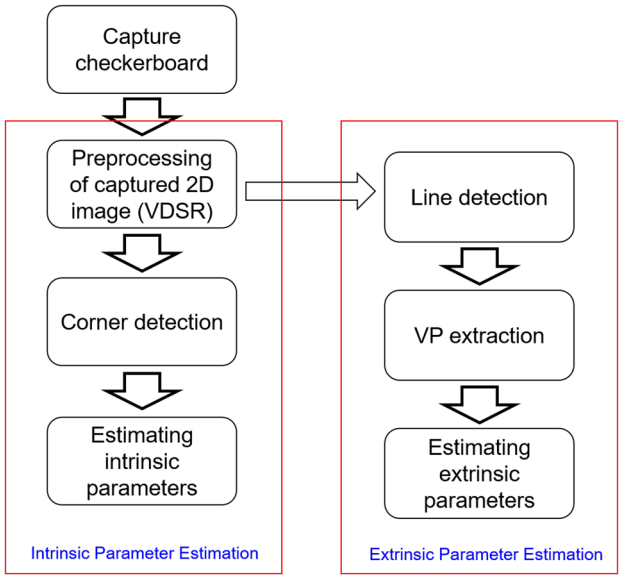

Figure 3 Overall flow diagram of estimating the intrinsic and the extrinsic parameters of the camera.

such as corner detection or line detection can be performed in reliable manner. Once the image are captured, calibration process is categorized into two tasks, the one is estimating the intrinsic parameters and the other one is estimating the extrinsic parameters. Typically, the intrinsic parameters are composed of the focal length, principal point (center coordinates of 2D image plane, and it intersects with the ray starting from optical center) and skew factor. The intrinsic parameters provide relationship between 2D coordinates of an image and 3D coordinates of a scene. Thus, accurate estimation of the intrinsic parameters is one of the most important factors in 3D reconstruction, depth estimation, 3D modeling, etc. Estimation of the intrinsic parameters stars from acquisition of 2D image pixels that is a projection of a 3D points of real world scene. Accurate detection of feature points in 2D image is important because detected image pixel is directly applied to mathematical model that establishes a relationship between 2D and 3D points. Usually, corner points are used as feature points, and numerous algorithms have been introduced for

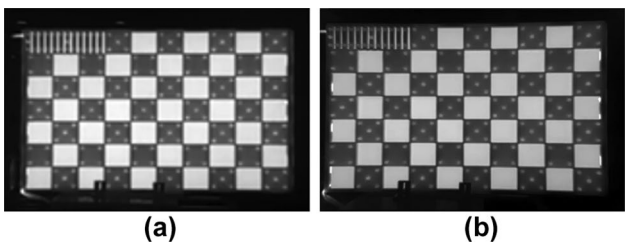

Figure 4 **a** An example of captured checkerboard image (25 °C). **b** An example of captured checkerboard image(45 °C).

accurate corner detection [36, 37]. Image quality also affects to performance of corner detection, so low-resolution to high-resolution mapping (LR to HR mapping) with convolutional neural network(CNN) is employed to generate high quality image. In this work, VDSR(Very Deep Super Resolution) is employed to generate high quality image and the algorithm shows better performance by showing high speed of convergence [38]. After performing image enhancement, edge detection was performed as in the normal calibration process. We also uses grid pattern (object is composed of squares) for calibration and we obtained intrinsic parameters by general calibration method. The relationship between 2D pixel and 3D point coordinates are calculated with iterative method for optimization. Besides the estimation of the intrinsic parameters, in this work, extrinsic parameters are estimated using different approach from the exited calibration methods. In the first, vertical and horizontal lines are detected. All of the horizontal and the vertical lines are straight and parallel each other in 3D space. However, projection of the lines in 2D space does not preserve parallelism, and the intersection point of the parallel lines in 3D space is projected on to a point in 2D space, called *vanishing point*(VP). As mentioned above (also shown in Fig. 2), there is few overlap between different viewpoints, so usual approach used in stereo vision does not work well in our case. The camera system suffers from feature matching, so disparity estimation is also difficult. Thus, this work fully exploits VPs. Based on VPs in 2D image, rotation and translation is determined. The next sections(Sections 4 and 5), detail the approach to determination of the intrinsic and the extrinsic parameters.

4 Intrinsic Parameters

Among the methods of image enhancement, low-resolution(LR) image based high-resolution(HR) image generation can be achieved using single image super resolution(SISR) method [39, 40]. Conventional method of LR to HR employs bilinear interpolation, Lanczos resampling or neighborhood embedding [41, 42]. Sparse encoding method uses compact dictionary trained by sparse signal representation [43]. Recently, CNN based image enhancement has been of interest, and contributes to significant improvement [44]. This work employs VDSR that shows superior performance compared to super-resolution CNN [45] in that VDSR has larger number of hidden layers and uses larger receptive field to utilize more image information. In addition VDSR shows good performance in case of high scale image by residual learning and high learning rate that leads to high convergence speed. While SRCNN works for single scale, VDSR works for multi scale and single network model. Once checkerboard is captured, we generate LR image as shown in Fig. 5

LR and HR images have high similarity, residual learning enables us to simply use VDSR. In VDSR, only Y channel is used, difference between HR image and Y channel image that is from highly scaled LR is trained. Y-channel image and generated HR image are shown in Fig. 6

As shown in Fig. 6, HR image is achieved by training difference between upscaled Y-channel of LR image and HR image. Once the processing of an image is performed, the next procedure is corner detection. Since thermal camera captures an object, the special checkerboard that emits heat is used. To detect corners, gradient based corner detection is used. The intrinsic parameters are estimated using *Levenberg-Marquardt*(LM) algorithm is employed [46]. LM algorithm is one of the most popular methods in nonlinear least squares problems. Estimation of the intrinsic problem can be formulated as following: $W[x, y, 1]^T = \mathbf{K}[\mathbf{R}|\mathbf{t}][X, Y, Z, 1]^T$, where W is a non-zero scaling factor (we can set this 1), $\mathbf{R}$ and t are rotation and translation matrices, respectively. $\mathbf{K}$ is the intrinsic parameter matrix, and $[\cdot]^T$ is a transpose operator. $\mathbf{K}$ includes the parameters, focal length, principal points and skewness factor (this is sometimes assumed to be zero). Our goal is to find all of the elements of $\mathbf{K}$, and LM method applies to this problem. In the $(k+1)^{th}$ iteration, $\mathbf{K}_{k+1}$ is calculated by the equation written by

$$\mathbf{K}_{k+1} = \mathbf{K}_k - (\mathbf{J}_r^T W \mathbf{J}_r)^{-1} \mathbf{J}_r^T W r(\mathbf{K}_k), \tag{5}$$

where $\mathbf{J}_r$ represents a *Jacobian* of $\mathbf{J}_r(\mathbf{K_k})$, and $r(\mathbf{K}_k)$ is a difference between the estimated intrinsic matrix in the k^{th} and the $(k+1)^{th}$ iteration. Since the number of elements of $\mathbf{K}$ is six (or five), we need at least five pairs of 2D and 3D points of the chekerboard to find the intrinsic parameters. LM method works similar to the gradient-descent algorithm, but LM shows lower possibility of divergence than the one of gradient-descent algorithm (LM is also called damped least-squares(DLS) method). The performance of the accuracy of the intrinsic parameters is affected by the number of captured images. However, the results show that the accuracy saturates once a number of images is larger than a specific number. For example, more than 5 captures (or planes) does not show significant improvement of accuracy (This is similar to the results reported in [5]). In addition, if the estimation work employs deep neural network model, a number of images can be reduced.

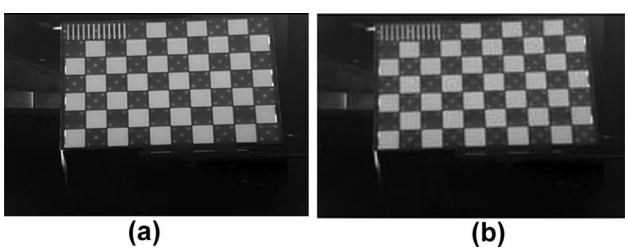

Figure 5 **a** An example of captured checkerboard image (original resolution). **b** An example of captured checkerboard image (low resolution).

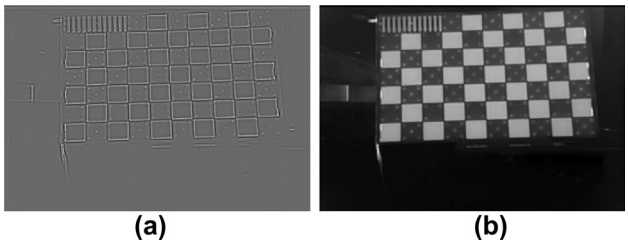

Figure 6 **a** An example of Y-channel image (upscaled from LR image. **b** An example of HR image.

5 Extrinsic Parameters

The extrinsic parameters are composed of rotation and translation. The extrinsic parameters can be represented using 3×4 matrix (see Eqs. (1), (2) and (4)). Since viewpoints have few overlapped regions (see Fig. 7), it is difficult to employ usual procedures of feature matching of stereo vision method. Since the system does not enable us to perform correspondence matching, different approach, vanishing points(VPs) based one, is considered in the course of estimating the extrinsic parameters.

VPs can be detected in an image of a 3D scene that has parallel lines. If there are parallel lines in three orthogonal directions, theoretically, three VPs are acquired. To achieve VPs in perfect manner, detection of parallel lines should be extracted and the lines intersect at single point. However, perfect acquisition of single VP in each direction is difficult due to the existence of noise in an image, lens distortion, etc. In this paper, optimal selection of VPs are carried out by finding intersection of multiple straight lines. For example, VP is simply found by finding intersection of two lines as shown in Fig. 8

Two parallel lines in a 2D image intersect at single point (x_i, y_i) that is corresponding to infinite point in 3D space.

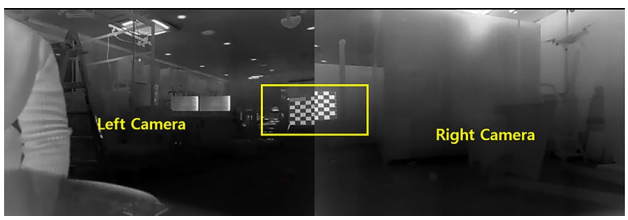

Figure 7 The camera system has few overlapped regions that leads to difficulties in employing usual procedures as stereo vision system does.

Given pixel coordinates of two lines, (x_i, y_i) can be simply found. Line 1 and Line 2 can be mathematically modeled as follows :

$$y = \frac{y_1 - y_i}{x_1 - x_i}(x - x_i), \tag{6}$$

$$y = \frac{y_2 - y_i}{x_2 - x_i}(x - x_i). \tag{7}$$

In addition to the points (x_1, y_1) and (x_2, y_2), we are given more 2D points in the images, leading to finding intersection point, that is called vanishing point(VP). At the most, three VPs can be extracted, each of which is a intersection of parallel lines in three directions, x, y and z direction. In other words, three mutually orthogonal directions are used to extract three VPs. These VPs can be used to estimate the extrinsic parameters, rotation matrix and translation vector. As well known, 2D ($p_i = \lambda(u_i, v_i, 1)$) and 3D real-world point ($P_i = (X_i, Y_i, Z_i, 1)$) has a following relationship (λ is a non-zero constant and it can be assumed to be 1).

$$\lambda \mathbf{m} = \mathbf{PM}, \tag{8}$$

where $\mathbf{m}$, $\mathbf{M}$ and $\mathbf{P}$ are 2D and 3D points, and *the projection matrix*, respectively, and Eq. (5) can be rewritten as

$$\lambda \begin{bmatrix} u_i & v_i & 1 \end{bmatrix}^T = \begin{bmatrix} p_{11} & p_{12} & p_{13} & p_{14} \\ p_{21} & p_{22} & p_{23} & p_{24} \\ p_{31} & p_{32} & p_{33} & p_{34} \end{bmatrix} \begin{bmatrix} X_i & Y_i & Z_i & 1 \end{bmatrix}^T \tag{9}$$

The projection matrix, $\mathbf{P}$ has a 11 dof(degrees of freedom) and it can be decomposed into the intrinsic and the extrinsic camera parameters. Thus, $\mathbf{P}$ can be written as

$$\mathbf{P} = \mathbf{M}_{in}\mathbf{M}_{ex}, \tag{10}$$

where $\mathbf{M}_{in}$ (3×3 matrix) and $\mathbf{M}_{ex}$ (3×4 matrix) are the intrinsic and the extrinsic parameters. $\mathbf{P}$ also can be written as

$$\mathbf{P} = \mathbf{M}_{in}[\mathbf{R}|\mathbf{t}], \tag{11}$$

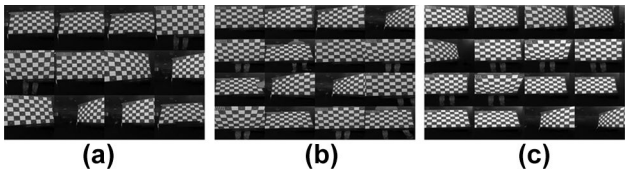

Figure 9 **a** Images from viewpoint 1. **b** Images from viewpoint 2. **c** Images from viewpoint 3.

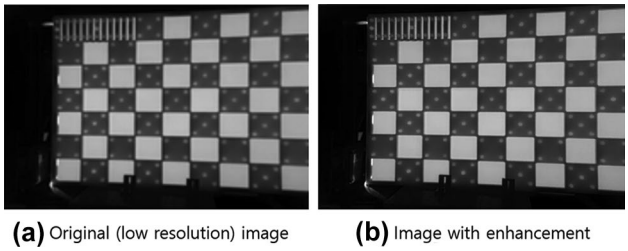

Figure 10 Result of an image with quality enhancement.

where $\mathbf{R}$ is a 3×3 rotation matrix and $\mathbf{t}$ is a 3×1 translation vector. Provided sufficient number of a pair of matched 2D points and the corresponding 3D points in the checkerboard, Eqs. (5) and (11) can be solved to find the optimal solution. Unless sufficient number of the points, traditional method cannot find the intrinsic and the extrinsic parameters. In this work, it is difficult to acquire pairs of 2D matched points because the camera system does not provide the same image of a target 3D scene. Instead of using matched points, vanishing points are fully exploited in this paper. Even though insufficient number of the matched points are provided, parallel lines definitely provides vanishing point. Multiple number of VPs are extracted and the corresponding 3D points are already known by projective geometry. Let $(u_i, v_i, 1)$ denote the pixel coordinate (homogeneous coordinate system is used in this paper) of a vanishing point, then $(X_i, Y_i, Z_i, 1)$ is defined as a 3D point at infinity. Using the Eq. (5) or (11), three sets of VPs theoretically provide sufficient information to find the extrinsic parameters. Since the intrinsic parameters are estimated in the previous section (Section 4), this

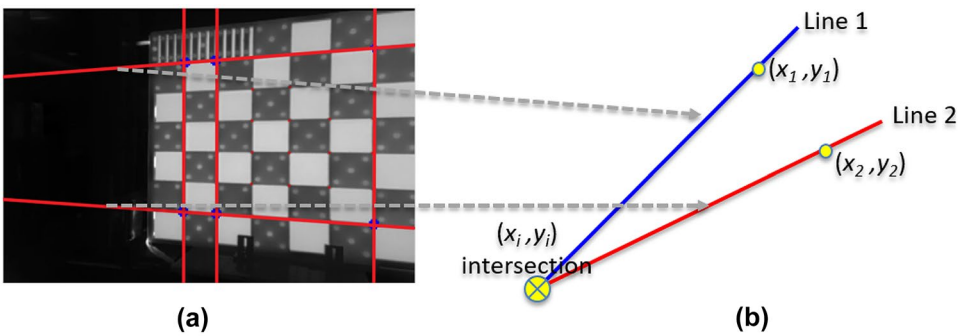

Figure 8 **a** Extraction of parallel lines. **b** Intersection of two lines.

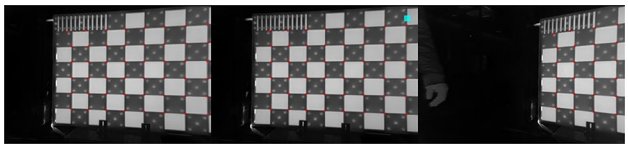

Figure 11 Results of corner detection of images with quality enhancement.

section chiefly deals with estimating the extrinsic parameters. Given pixel coordinates of the VPs, the corresponding 3D coordinates are [1, 0, 0, 0] and [0100] for horizontal and vertical VPs, respectively. Since we have VPs in two directions, i.e., vertical(x direction) and horizontal (y direction), pseudo inverse matrix needs to be calculated from Eq. (2). In the next section, to substantiate the proposed method, experimental results are provided.

6 Experimental Results

In the experiments, the intrinsic and the extrinsic parameters are estimated separately. To estimate the intrinsic parameters, multiple number of images are captured using a thermal camera. Since three points belong to a single thermal camera system, the parameters are estimated for each viewpoint. Images of the checkerboard captured by thermal camera are shown in Fig. 9

Once images are acquired, prior to corner detection, quality enhancement using VDSR (very deep super resolution) [38] is performed. An example of a result of quality enhancement is shown in Fig. 10, followed by the results of corner detection (Fig. 11).

Since all of the viewpoints are independent each other, the procedures to estimate the intrinsic parameters are identical. Once the intrinsic parameters are calculated, accuracy is evaluated by calculating the reprojection error that is a distance between 2D points of an image and the corresponding projected image points of a 3D real-world points. Let $\mathbf{x}$ and $\mathbf{P}(\mathbf{X})$ denote 2D point and a projected 3D point into an image plane, reprojection error can be represented as $E_{rp} = |x - P(X)|$, where $\mathbf{x} = (x_1, x_2, ..., x_N)$ and $\mathbf{X} = (X_1, X_2, ..., X_N)$, respectively. $\mathbf{P}(\mathbf{X})$ represents a projection of 3D points into 2D image plane. Thus, the goal of the calibration is to minimize E_{rp}. Reprojection error for each viewpoint is shown in Fig. 12.

Table 1 Estimated intrinsic parameters.

focal length (f_x)	**focal length** (f_y)	**principal point** (p_x, p_y)
598.2455 (pixels)	520.6282 (pixels)	(371.2485, 238.4712) (pixels)

The estimated intrinsic parameters are in Table 1

In the proposed approach in this paper, in addition to the existed method of the calibration, VDSR based image enhancement and finding optimal temperature have been carried out. It is difficult to directly compare the result to the extisted work because the experimental environment is different and a type of camera is also different. However, the reprojection error is smaller than 1 pixel out of the image size (1125×750 pixels). As very well known, in the course of estimating the intrinsic parameters, lens distortion, external and internal temperature, etc. affect to the estimation results. This paper has employed the exited approach that use multiple images of checkerboard images, and the results have been acquired by iterative optimization. The extrinsic parameters are estimated based on detected VPs. Fig. 13 shows VPs extracted from the captured image.

Since the viewpoints have different rotation angle, this section focuses on estimating relative rotation between viewpoints. In the experiments, viewpoint has been rotated by 2 degree, i.e., this is a ground-truth, and the estimated result has been compared to the true value. Since the rotation has been performed along with y-direction, the results are expected to show zero degree in x and z directions. The rotation results show that, in average, $R_x = 0.0661$, $R_y = 1.5947$, $R_z = 5.22 \times 10^{-5}$. For each viewpoint, for each ground-truth, the estimated results are described in Table 2.

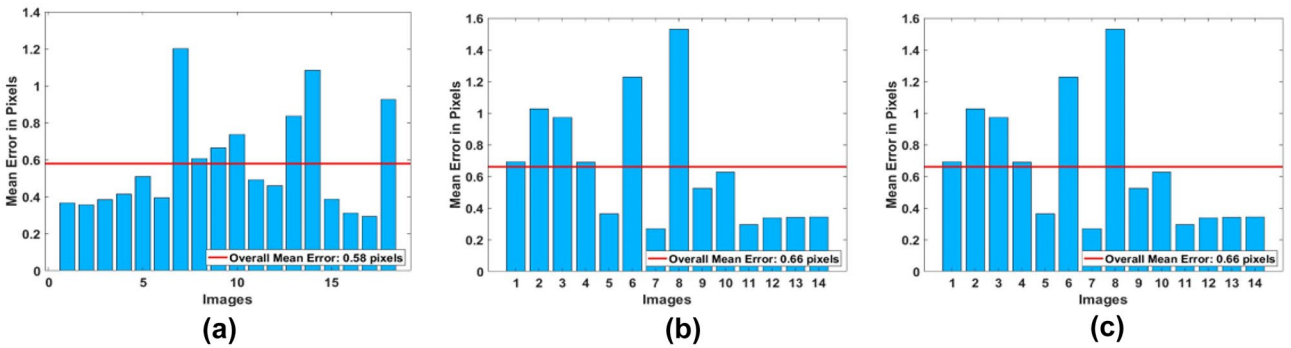

Figure 12 Reprojection error for each viewpoint. **a** Viewpoint 1. **b** Viewpoint 2. **c** Viewpoint 3.

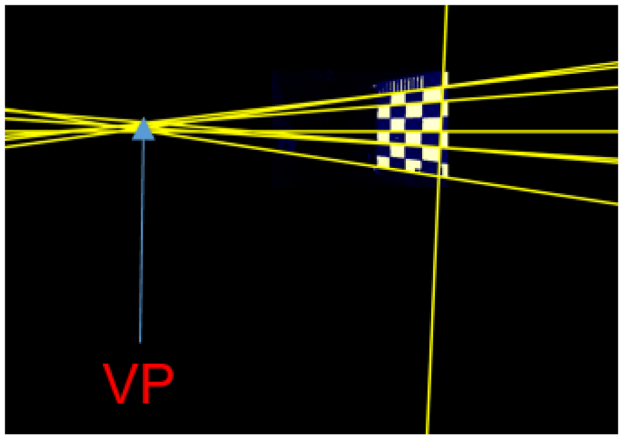

Figure 13 Vanishing point detected in 2D projected image of a 3D scene.

Table 2 Estimated rotation of a camera.

Ground-truth	R_x(deg)	R_y(deg)	R_z(deg)
$R_y = 2, R_x = R_z = 0$	-0.0056	1.5947	5.22×10^{-5}
$R_y = 5, R_x = R_z = 0$	0.070	4.4405	3.85×10^{-5}

As shown in the results (Table 2), the accuracy is worse when the truth value is larger. However, the accuracy of R_z shows reliable result. Current research on the calibration is focusing on increasing the accuracy of the estimation. In addition to the experiments of the estimation of relative rotations, VP based estimation of relative rotation by varying the rotation angle by 2° (degree). The results are shown in Table 3.

Table 4 shows the comparison results with the other work that have proposed estimation of camera rotation. To perform comparison, accuracy rate (out of 100 percentage) is used. The accuracy in average is presented for comparison.

Table 3 Estimated rotation of a camera by varying an angle.

Ground-truth	R_x(deg)	R_y(deg)	R_z(deg)
$R_y = 0, R_x = R_z = 0$	-0.0205	0.0164	−0.0180
$R_y = 2, R_x = R_z = 0$	-0.0222	2.1124	5.22×10^{-5}
$R_y = 4, R_x = R_z = 0$	-0.0651	3.9194	3.85×10^{-5}
$R_y = 6, R_x = R_z = 0$	-0.0321	5.9131	1.315×10^{-5}
$R_y = 8, R_x = R_z = 0$	-0.0001	8.1981	1.833×10^{-5}
$R_y = 10, R_x = R_z = 0$	-0.0563	11.0015	-1.570×10^{-5}
$R_y = 14, R_x = R_z = 0$	-0.0649	14.0897	-4.214×10^{-5}
$R_y = 16, R_x = R_z = 0$	-0.0206	17.0254	-1.802×10^{-5}
$R_y = 20, R_x = R_z = 0$	-0.0315	20.5400	0.2018
$R_y = 24, R_x = R_z = 0$	-0.0003	25.2339	−1.0000

Table 4 Comparison results with the other results.

	Accuracy (Rotation error in percentage or degree)
Proposed	0.6%(0.0897*deg*), 0.43*deg* (in average)
Lecrosnier et al. [47]	0.15*deg*
Zhou and Deng [48]	12.03*deg*
Bazin et al. [21]	0.3*deg*
Chen et al. [49]	3.96*deg*
Wang et al. [50]	1.152*deg*
Liu et al. [51]	1.51*deg*

7 Conclusion

This paper has presented the approach to camera calibration using a thermal camera system of three-viewpoints. Although the procedures of the calibration is similar to the existed ones, image enhancement and vanishing point based estimation of rotation, the most contribution of this paper, is desired to accomplish the results. Contrary to the usual stereo camera system, our camera system does not provide same feature points that are to be used for correspondence matching. Without correspondence matching, usual calibration method cannot be employed. Instead of using correspondence matching, vanishing points based estimation of the extrinsic parameters is presented in this paper. The approach is very simple but the estimation process suffers from the ill-posed problem leading to optimization process. This paper has shown the preliminary results that show possibilities of performing camera calibration with few correspondence matching (or no correspondence matching in case of extreme cases). In the future, stitching to generate panorama images using a thermal camera system with accurate estimation of the calibration parameters will be performed. For the limitation, the checkerboard we used in this experiment was manufactured separately for the camera, and unlike the general checkerboard, it is large in size and sensitive to heat. Due to the size and sensitivity problems, the calibration accuracy was affected, which acted as a limit to the accuracy.

Funding This work was supported by Basic Science Research Program through the National Research Foundation of Korea(NRF) funded by the Ministry of Education(2022R1I1A3069352).

Data Availability All of the data is available upon the request.

Declarations

Competing Interest The authors have no competing interests to declare that are relevant to the content of this article.

References

1. Faugeras, O., & Faugeras, O. A. (1993). Three-dimensional computer vision: a geometric viewpoint. MIT press.
2. Zanuttigh, P., Marin, G., Dal Mutto, C., Dominio, F., Minto, L., & Cortelazzo, G. M. (2016). Time-of-flight and structured light depth cameras. *Technology and Applications*, 978-3.
3. Batlle, J., Mouaddib, E., & Salvi, J. (1998). Recent progress in coded structured light as a technique to solve the correspondence problem: a survey. *Pattern Recognition, 31*(7), 963–982.
4. Zhang, J., Yu, H., Deng, H., Chai, Z., Ma, M., & Zhong, X. (2018). A robust and rapid camera calibration method by one captured image. *IEEE Transactions on Instrumentation and Measurement, 68*(10), 4112–4121.
5. Zhang, Z. (2000). A flexible new technique for camera calibration. *IEEE Transactions on pattern analysis and machine intelligence, 22*(11), 1330–1334.
6. Faugeras, O. D., Luong, Q. T., & Maybank, S. J. (1992, May). Camera self-calibration: Theory and experiments. In European conference on computer vision (pp. 321-334). Springer, Berlin, Heidelberg.
7. Hartley, R. I. (1994, May). Self-calibration from multiple views with a rotating camera. In European Conference on Computer Vision (pp. 471-478). Springer, Berlin, Heidelberg.
8. Heikkilä, J. (2000). Geometric camera calibration using circular control points. *IEEE Transactions on pattern analysis and machine intelligence, 22*(10), 1066–1077.
9. Lopez, M., Mari, R., Gargallo, P., Kuang, Y., Gonzalez-Jimenez, J., & Haro, G. (2019). Deep single image camera calibration with radial distortion. In Proceedings of the IEEE/CVF Conference on Computer Vision and Pattern Recognition (pp. 11817-11825).
10. Rahimi, A., Dunagan, B., & Darrell, T. (2004). Simultaneous calibration and tracking with a network of non-overlapping sensors. IEEE Computer Society Conference on Computer Vision and Pattern Recognition Vol. 1. IEEE.
11. Haralick, R. M. (1989). Determining camera parameters from the perspective projection of a rectangle. *Pattern Recognition, 22*(3), 225–230.
12. Caprile, B., & Torre, V. (1990). Using vanishing points for camera calibration. *International Journal of Computer Vsion, 4*(2), 127–139.
13. Shigang, L., Tsuji, S., & Imai, M. (1990, January). Determining of camera rotation from vanishing points of lines on horizontal planes. In Proceedings Third International Conference on Computer Vision (pp. 499-500). IEEE Computer Society.
14. Guillou, E., Meneveaux, D., Maisel, E., & Bouatouch, K. (2000). Using vanishing points for camera calibration and coarse 3D reconstruction from a single image. *The Visual Computer, 16*(7), 396–410.
15. Chen, W., & Jiang, B. C. (1991). 3-D camera calibration using vanishing point concept. *Pattern Recognition, 24*(1), 57–67.
16. Wang, L. L., & Tsai, W. H. (1991). Camera calibration by vanishing lines for 3-D computer vision. *IEEE Transactions on Pattern Analysis and Machine Intelligence, 13*(4), 370–376.
17. Dhome, M., Richetin, M., Lapresté, J. T., & Rives, G. (1988, June). The inverse perspective problem from a single view for polyhedra location. In Proceedings CVPR'88: The Computer Society Conference on Computer Vision and Pattern Recognition (pp. 61-66). IEEE.
18. Cipolla, R., Drummond, T., & Robertson, D. P. (1999, September). Camera Calibration from Vanishing Points in Image of Architectural Scenes. In BMVC (Vol. 99, pp. 382-391).
19. Orghidan, R., Salvi, J., Gordan, M., & Orza, B. (2012, September). Camera calibration using two or three vanishing points. In 2012 Federated Conference on Computer science and information systems (FedCSIS) (pp. 123-130). IEEE.
20. Lee, J. K., & Yoon, K. J. (2015). Real-time joint estimation of camera orientation and vanishing points. In Proceedings of the IEEE Conference on Computer Vision and Pattern Recognition (pp. 1866-1874).
21. Bazin, J. C., Demonceaux, C., Vasseur, P., & Kweon, I. (2012). Rotation estimation and vanishing point extraction by omnidirectional vision in urban environment. *The International Journal of Robotics Research, 31*(1), 63–81.
22. Bazin, J. C., Seo, Y., Demonceaux, C., Vasseur, P., Ikeuchi, K., Kweon, I., & Pollefeys, M. (2012, June). Globally optimal line clustering and vanishing point estimation in manhattan world. In 2012 IEEE Conference on Computer Vision and Pattern Recognition (pp. 638-645). IEEE.
23. Elloumi, W., Treuillet, S., & Leconge, R. (2017). Real-time camera orientation estimation based on vanishing point tracking under manhattan world assumption. *Journal of Real-Time Image Processing, 13*(4), 669–684.
24. Antunes, M., Barreto, J. P., Aouada, D., & Ottersten, B. (2017). Unsupervised vanishing point detection and camera calibration from a single manhattan image with radial distortion. In Proceedings of the IEEE Conference on Computer Vision and Pattern Recognition (pp. 4288-4296).
25. Chang, H., & Tsai, F. (2017). Vanishing point extraction and refinement for robust camera calibration. *Sensors, 18*(1), 63.
26. Lee, S. J., & Hwang, S. S. (2020). Fast and accurate self-calibration using vanishing point detection in manmade environments. *International Journal of Control, Automation and Systems, 18*(10), 2609–2620.
27. Jang, J., Jo, Y., Shin, M., & Paik, J. (2020). Camera orientation estimation using motion-based vanishing point detection for advanced driver-assistance systems. *IEEE Transactions on Intelligent Transportation Systems, 22*(10), 6286–6296.
28. Sun, J., Wang, H., & Zhu, X. (2021). A fast underwater calibration method based on vanishing point optimization of two orthogonal parallel lines. *Measurement, 178*, 109305.
29. Pagel, F. (2010, June). Calibration of non-overlapping cameras in vehicles. *In 2010 IEEE Intelligent Vehicles Symposium* (pp. 1178-1183). IEEE.
30. Esquivel, S., Woelk, F., & Koch, R. (2007, September). Calibration of a multi-camera rig from non-overlapping views. *In Joint Pattern Recognition Symposium* (pp. 82-91). Springer, Berlin, Heidelberg.
31. Kumar, R. K., Ilie, A., Frahm, J. M., & Pollefeys, M. (2008, June). Simple calibration of non-overlapping cameras with a mirror. *In 2008 IEEE Conference on Computer Vision and Pattern Recognition* (pp. 1-7). IEEE.
32. Van Crombrugge, I., Penne, R., & Vanlanduit, S. (2020). Extrinsic camera calibration for non-overlapping cameras with Gray code projection. *Optics and Lasers in Engineering, 134*, 106305.
33. Lébraly, P., Deymier, C., Ait-Aider, O., Royer, E., & Dhome, M. (2010, October). Flexible extrinsic calibration of non-overlapping cameras using a planar mirror: Application to vision-based robotics. *In 2010 IEEE/RSJ International Conference on Intelligent Robots and Systems* (pp. 5640-5647). IEEE.
34. Huang, H., Li, N., Guo, H., Chen, Y. L., & Wu, X. (2015, April). Calibration of non-overlapping cameras based on a mobile robot. *In 2015 5th International Conference on Information Science and Technology (ICIST)* (pp. 328- 333). IEEE.
35. Xia, R., Hu, M., Zhao, J., Chen, S., Chen, Y., & Fu, S. (2018). Global calibration of non-overlapping cameras: State of the art. *Optik, 158*, 951–961.
36. Chen, X., Liu, L., Song, J., Li, Y., & Zhang, Z. (2018). Corner detection and matching for infrared image based on double ring mask and adaptive SUSAN algorithm. *Optical and Quantum Electronics, 50*(4), 1–10.
37. Dutta, A., Kar, A., & Chatterji, B. N. (2008). Corner detection algorithms for digital images in last three decades. *IETE Technical Review, 25*(3), 123–133.

38. Kim, J., Lee, J. K., & Lee, K. M. (2016). Accurate image super-resolution using very deep convolutional networks. *In Proceedings of the IEEE conference on computer vision and pattern recognition* (pp. 1646-1654).
39. Kumar, N., & Sethi, A. (2016). Fast learning-based single image super-resolution. *IEEE Transactions on Multimedia, 18*(8), 1504–1515.
40. Yang, W., Zhang, X., Tian, Y., Wang, W., Xue, J. H., & Liao, Q. (2019). Deep learning for single image super-resolution: A brief review. *IEEE Transactions on Multimedia, 21*(12), 3106–3121.
41. Duchon, C. E. (1979). Lanczos filtering in one and two dimensions. *Journal of Applied Meteorology and Climatology, 18*(8), 1016–1022.
42. Alonso-Fernandez, F., Farrugia, R. A., & Bigun, J. (2017). Iris super-resolution using iterative neighbor embedding. *In Proceedings of the IEEE Conference on Computer Vision and Pattern Recognition Workshops* (pp. 153-161).
43. Zeyde, R., Elad, M., & Protter, M. (2010, June). On single image scale-up using sparse-representations. *In International conference on curves and surfaces* (pp. 711-730). Springer, Berlin, Heidelberg.
44. Zhu, H., Xie, C., Fei, Y., & Tao, H. (2021). Attention mechanisms in CNN-based single image super-resolution: A brief review and a new perspective. *Electronics, 10*(10), 1187.
45. Dai, Y., Jin, T., Song, Y., Du, H., & Zhao, D. (2018, August). SRCNN-based enhanced imaging for low frequency radar. *In 2018 Progress in Electromagnetics Research Symposium (PIERS-Toyama)* (pp. 366-370). IEEE.
46. Moré, J. J. (1978). The Levenberg-Marquardt algorithm: implementation and theory. *In Numerical analysis* (pp. 105-116). Springer, Berlin, Heidelberg.
47. Lecrosnier, L., Boutteau, R., Vasseur, P., Savatier, X., & Fraundorfer, F. (2019). Camera pose estimation based on PnL with a known vertical direction. *IEEE Robotics and Automation Letters, 4*(4), 3852–3859.
48. Zhou, L., & Deng, Z. (2012, June). Extrinsic calibration of a camera and a lidar based on decoupling the rotation from the translation. *In 2012 IEEE Intelligent Vehicles Symposium* (pp. 642-648). IEEE.
49. Chen, K., Snavely, N., & Makadia, A. (2021). Wide-baseline relative camera pose estimation with directional learning. *In Proceedings of the IEEE/CVF Conference on Computer Vision and Pattern Recognition* (pp. 3258-3268).
50. Wang, P., Xu, G., Cheng, Y., & Yu, Q. (2019). Camera pose estimation from lines: a fast, robust and general method. *Machine Vision and Applications, 30*(4), 603–614.
51. Liu, Y., Chen, G., & Knoll, A. (2020). Globally optimal camera orientation estimation from line correspondences by bnb algorithm. *IEEE Robotics and Automation Letters, 6*(1), 215–222.